International Journal of Computational Fluid Dynamics, 2014
Vol. 28, Nos. 3–4, 91–105, http://dx.doi.org/10.1080/10618562.2014.911848

Taylor & Francis
Taylor & Francis Group

Model reduction for reacting flow applications

V.B. Nguyen[a], M. Buffoni[b], K. Willcox[c,*] and B.C. Khoo[d]

[a]*Department of Engineering Mechanics, Institute of High Performance Computing, Singapore, Singapore;* [b]*Power Device Simulations Group, ABB Switzerland Ltd., Corporate Research, Baden-Dättwil, Switzerland;* [c]*Department of Aeronautics and Astronautics, Massachusetts Institute of Technology, Cambridge, MA, USA;* [d]*Department of Mechanical Engineering, National University of Singapore, Singapore 117576, Singapore*

(*Received 2 December 2013; accepted 31 March 2014*)

A model reduction approach based on Galerkin projection, proper orthogonal decomposition (POD), and the discrete empirical interpolation method (DEIM) is developed for chemically reacting flow applications. Such applications are challenging for model reduction due to the strong coupling between fluid dynamics and chemical kinetics, a wide range of temporal and spatial scales, highly nonlinear chemical kinetics, and long simulation run-times. In our approach, the POD technique combined with Galerkin projection reduces the dimension of the state (unknown chemical concentrations over the spatial domain), while the DEIM approximates the nonlinear chemical source term. The combined method provides an efficient offline–online solution strategy that enables rapid solution of the reduced-order models. Application of the approach to an ignition model of a premixed H_2/O_2/Ar mixture with 19 reversible chemical reactions and 9 species leads to reduced-order models with state dimension several orders of magnitude smaller than the original system. For example, a reduced-order model with state dimension of 60 accurately approximates a full model with a dimension of 91,809. This accelerates the simulation of the chemical kinetics by more than two orders of magnitude. When combined with the full-order flow solver, this results in a reduction of the overall computational time by a factor of approximately 10. The reduced-order models are used to analyse the sensitivity of outputs of interest with respect to uncertain input parameters describing the reaction kinetics.

Keywords: model reduction; POD; DEIM; chemically reacting flows; partial differential equations

1. Introduction

Numerical simulation of reacting flows is important for studying and improving combustion processes, but is a computationally challenging task. The accurate modelling of combustion processes using detailed reaction mechanisms leads to stiff systems of differential equations with multiscale dynamics that take place over a large range of temporal and spatial scales, from very fast reactions that occur in a fraction of a second to the longer times scales present in the fluid dynamics. Therefore, fine spatial grids and small time steps are usually needed. In addition, a detailed chemistry model involves many chemical species and many reactions, which means that these models can quickly become large. Even with state-of-the-art simulation techniques (specialised numerical discretisation schemes and massively parallel implementations), design, control, and optimisation of these systems remains intractable for realistic engineering applications. To address these challenges, we develop a projection-based model reduction technique for reacting flows that reduces computational cost while maintaining accuracy.

Several methods have been developed over the past years to reduce the computational cost of evaluating the chemical source term. These methods include, among others, the quasi-steady-state approximation, the partial equilibrium approximation (Ramshaw 1980; Peters and Williams 1987), principal component analysis (Brown, Li, and Koszykowski 1997), intrinsic low-dimensional manifold (ILDM) (Maas and Pope 1992b, 1992a, 1994), and computational singular perturbation (CSP) (Lam 1993; Lam and Goussis 1994; Hadjinicolaou and Goussis 1999). The CSP method describes the system of ordinary differential equations (ODEs) governing the reaction source term at each grid point by a linear combination of CSP basis vectors. These vectors decompose the equations governing the chemistry into fast and slow modes. The species and reactions corresponding to fast modes are eliminated from the system in the following integration step. Thus, the system of equations becomes smaller and, since the small (fast) time scales have been removed, non-stiff. As a consequence, the solution of the reduced reaction term requires less computational effort at each time step. Furthermore, the CSP provides an iterative refinement algorithm to compute automatically an approximation to the ideal basis vectors that decouple the fast and slow subspaces. The algorithm is usually initialised using the eigenmodes of the Jacobian of the

* Corresponding author. Email: kwillcox@mit.edu

chemical source term. Similarly, the ILDM, a method based on a dynamical systems approach, separates automatically the slow and fast time scales. These scales are identified by analysing the local eigenvectors of the Jacobian of the reaction source term. The ILDM is usually applied in conjunction with a tabulating procedure that allows its use in CFD simulation codes. Although time-scale separation methods have been applied successfully in numerical simulations of reacting flows, their computational cost is usually still high when the number of chemical species and/or reactions is high. The ILDM and CSP methods both require for the identification of slow and fast spaces the analysis of the local Jacobian and its eigenvectors, which need to be updated many times. Moreover, these methods were developed for spatially homogeneous reactive systems described by ODEs rather than partial differential equations (PDEs) that model spatially inhomogeneous reacting flows.

In this paper, we focus instead on projection-based model reduction. In this context, the reduced models are obtained by performing Galerkin projection of the large-scale system of equations onto the space spanned by a small set of basis vectors. Different methods exist to construct the required basis vectors. Such methods include, for example, Krylov subspace methods (Gallivan, Grimme, and Van Dooren 1994, 1999; Feldmann and Freund 1995; Grimme 1997), balanced truncation (Gugercin and Antoulas 2004; Sorensen and Antoulas 2002), and proper orthogonal decomposition (POD) (Sirovich 1987; Holmes, Lumley, and Berkooz 1998). Galerkin projection combined with the POD technique has been successfully used in many areas such as fluid mechanics (Lucia, King, and Beran 2003; Ma and Karniadakis 2002; Buffoni et al. 2006) and structural mechanics (Amabili, Sarkar, and Païdoussis 2006; Kerschen et al. 2005). The method is able to obtain in many cases orders-of-magnitude reduction in the order of the system, since the dynamics of interest can often be represented by a small number of POD modes. The computation of the basis functions (POD modes) is straightforward; the POD modes are constructed as the span of a set of state solutions (snapshots). Such snapshots are computed by solving the large-scale system for selected values of parameters and selected inputs. However, in the case of nonlinear systems, the POD–Galerkin method leads to inefficient reduced models since the projected nonlinear term requires computations that scale with the dimension of the original large-scale problem.

Methods to approximate the projected nonlinear term in a POD reduced model include the missing point estimation technique (Astrid et al. 2008), which uses selected spatial sampling based on the theory of the gappy POD (Everson and Sirovich 1995). Another approach is the empirical interpolation method (EIM) (Barrault et al. 2004; Grepl et al. 2007), which uses a linear combination of empirical basis functions to approximate the projected nonlinear term. The coefficients of this expansion are determined

Table 1. DEIM algorithm used to compute the desired interpolation indices.

INPUT:	$[\mathbf{U}_k]_{k=1}^{L} \subset \mathbb{R}^M$ linearly independent
OUTPUT:	$\vec{p} = [p_1, \ldots, p_L]^T \in \mathbb{R}^L$
1:	$[\lvert\rho\rvert\, p_1] = \max(\lvert\mathbf{U}_1\rvert)$
2:	$\mathbf{U} = [\mathbf{U}_1], \quad \mathbf{P} = [\mathbf{e}_{p_1}, \quad \vec{p} = [p_1]]$
3:	for $k = 2$ to L do
4:	Solve $(\mathbf{P}^T\mathbf{U})\mathbf{c} = \mathbf{P}^T\mathbf{U}_k$ for c
5:	$\mathbf{r} = \mathbf{U}_k - \mathbf{U}\mathbf{c}$
6:	$[\lvert\rho\rvert \quad p_k] = \max(\lvert\mathbf{r}\rvert)$
7:	$\mathbf{U} \leftarrow [\mathbf{U} \quad \mathbf{U}_k], \mathbf{P} \leftarrow [\mathbf{P} \quad \mathbf{e}_{p_k}], \vec{p} \leftarrow [\vec{p}\, p_k]^T$
8:	end for

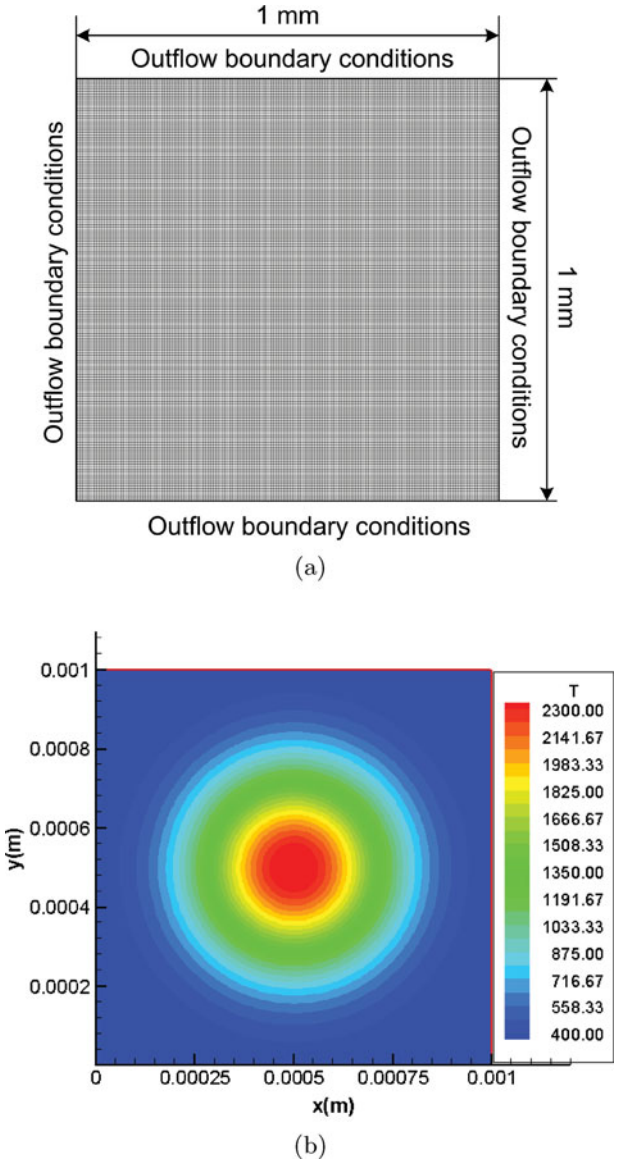

Figure 1. Problem setup: (a) domain discretisation and boundary conditions; (b) initial conditions.

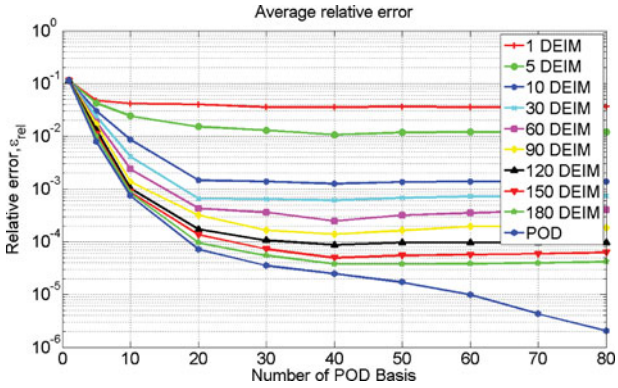

Figure 2. Average relative errors (2-norm) of the solution computed using the POD–DEIM reduced-order models with a varying number of POD basis vectors (K) and DEIM modes (L).

by interpolation. We use here the discrete empirical interpolation method (DEIM), a discrete variant of the EIM (Chaturantabut and Sorensen 2010). We show that a POD–DEIM reduced model can accurately represent chemical kinetics, while providing significant speedups in computation times.

Section 2 of this paper introduces the reacting flow model and numerical solution approach. Section 3 presents the POD–DEIM model reduction approach. Section 4 presents an application of the model reduction method to a premixed flame model and Section 5 concludes the paper.

2. Reacting flow model

The combustion process is modelled by a detailed chemical kinetics model of N_s species and N_r elementary reactions. All gas species are considered thermally perfect, and we assume the equation of state (EOS) of perfect gases is applicable. We assume that there is no body force acting on the chemical species and that there is no external heat source

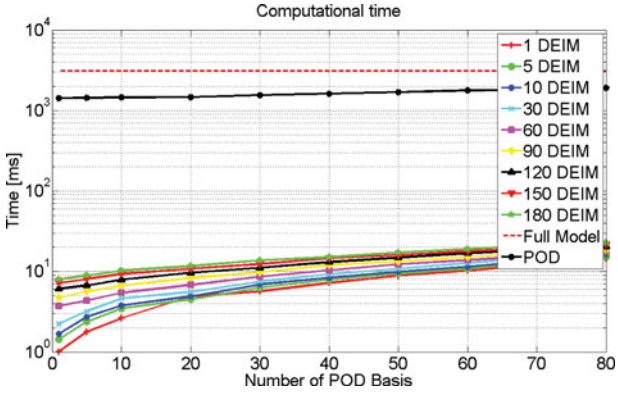

Figure 3. Comparison of the average computational simulation time between the POD–DEIM reduced-order model, the POD model, and the full model for one time step of chemical kinetics.

(sparks, etc.). With these assumptions, the governing equations for the evolution of a perfect gas mixture involving N_s species and N_r reversible chemical reactions can be written, in Cartesian coordinates, in the form

$$\frac{\partial \mathbf{U}}{\partial t}+\frac{\partial \mathbf{F}(\mathbf{U})}{\partial x}+\frac{\partial \mathbf{G}(\mathbf{U})}{\partial y}=\frac{1}{Re}\left(\frac{\partial \mathbf{H}(\mathbf{U})}{\partial x}+\frac{\partial \mathbf{T}(\mathbf{U})}{\partial y}\right)+\mathbf{S}(\mathbf{U}), \tag{1}$$

where

$$\mathbf{U}=\left[\rho,\rho u,\rho v,\rho E,\rho Y_1,\ldots,\rho Y_{N_s}\right]^T, \tag{2a}$$

$$\mathbf{F}=\left[\rho u,\rho u^2+p,\rho uv,(E+p)u,\rho uY_1,\ldots,\rho uY_{N_s}\right]^T, \tag{2b}$$

$$\mathbf{G}=\left[\rho v,\rho uv,\rho v^2+p,(E+p)v,\rho vY_1,\ldots,\rho vY_{N_s}\right]^T, \tag{2c}$$

$$\mathbf{H}=\left[0,\tau_{xx},\tau_{xy},A_x,\frac{1}{S_{ck}}\mu\frac{\partial Y_1}{\partial x},\ldots,\frac{1}{S_{ck}}\mu\frac{\partial Y_{N_s}}{\partial x}\right]^T, \tag{2d}$$

$$\mathbf{T}=\left[0,\tau_{yx},\tau_{yy},A_y,\frac{1}{S_{ck}}\mu\frac{\partial Y_1}{\partial y},\ldots,\frac{1}{S_{ck}}\mu\frac{\partial Y_{N_s}}{\partial y}\right]^T, \tag{2e}$$

$$\mathbf{S}=\left[0,0,0,0,\dot{\omega}_1(p,T,Y_1,\ldots,Y_{N_s}),\ldots,\dot{\omega}_{N_s}(p,T,Y_1,\ldots,Y_{N_s})\right]^T, \tag{2f}$$

$$A_x=u\tau_{xx}+v\tau_{xy}+\frac{1}{(\gamma-1)M^2Pr}\left(\mu\frac{\partial T}{\partial x}\right)+\frac{1}{(\gamma-1)M^2}\sum_{k=1}^{N_s}\left(h_k\frac{\mu}{S_{ck}}\frac{\partial Y_k}{\partial x}\right), \tag{3a}$$

$$A_x=u\tau_{yx}+v\tau_{yy}+\frac{1}{(\gamma-1)M^2Pr}\left(\mu\frac{\partial T}{\partial y}\right)+\frac{1}{(\gamma-1)M^2}\sum_{k=1}^{N_s}\left(h_k\frac{\mu}{S_{ck}}\frac{\partial Y_k}{\partial y}\right), \tag{3b}$$

where ρ is the density of the mixture, u and v are the velocity components, E is the total energy, $Y_1,\ldots,Y_{N_s}$ are the mass fractions of the species, p is the pressure of the mixture, T is the temperature of the mixture, $\dot{\omega}$ is the mass production rate of species, $S_{ck}=\mu/(\rho D_k)$ is the Schmidt number, Re is the Reynolds number, M is the Mach number, $Pr=c_p\mu/\lambda$ is the Prandtl number, N_s is the total number of species, and τ_{ij} is the viscous stress tensor expressed as

$$\tau_{ij}=\mu\left[\frac{\partial u_i}{\partial x_j}+\frac{\partial u_j}{\partial x_i}-\frac{2}{3}\frac{\partial u_k}{\partial x_k}\delta_{ij}\right]. \tag{4}$$

The enthalpies h_k, the specific heat capacity at constant pressure c_p, the Gibbs free energy, the dynamic viscosity

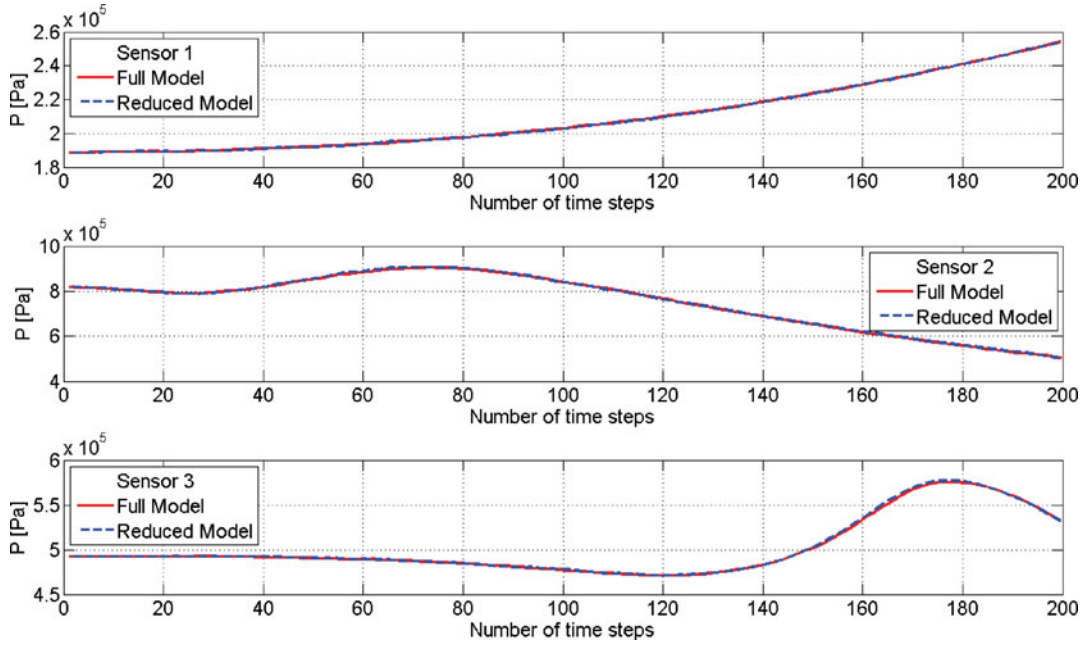

Figure 4. Comparison of solutions of the pressure evolution at three sensor locations between the POD–DEIM reduced model of size $K = 40$, $L = 60$ and the full model of size $M = 91,809$.

μ, thermal conductivity λ, and diffusion coefficients D_k for species k and for the mixture are computed using polynomial fits and transport databases from CEA (McBride and Sanford 1994, 1996) and JANAF (Stull and Prophet 1971; Chase 1998), and classical kinetics theory.

The mass production rate, $\dot{\omega}$, of species k in the source term of Equation (2f) is computed by

$$\dot{\omega}_k = W_k \sum_{i=1}^{N_r} \left(\nu''_{ki} - \nu'_{ki}\right)\left(\alpha_{ki}[X_k]\right) \times \left\{ K_{f,i} \prod_{k=1}^{N_s} [X_k]^{\nu'_{ki}} - K_{b,i} \prod_{k=1}^{N_s} [X_k]^{\nu''_{ki}} \right\}, \quad (5)$$

where ν'_{ki} and ν''_{ki} are the chemical stoichiometric coefficients of the reactant and the product for species k in reaction i, respectively. $K_{f,i}$ and $K_{b,i}$ are the forward and backward coefficients of the reaction computed through the Arrhenius law for the state value of pressure, temperature, and mole fraction, W_k is the molecular weight of species k, and $[X_k]$ is the molar concentration of species k in reaction i. This molar concentration of species k is defined by $[X_k] = \rho Y_k / W_k$, and α_{ki} are the third-body coefficient factors of species k in reaction i.

We use an operator-splitting scheme to separate the governing equations (1) into a fluid dynamics part:

$$\frac{\partial \mathbf{U}}{\partial t} + \frac{\partial \mathbf{F}(\mathbf{U})}{\partial x} + \frac{\partial \mathbf{G}(\mathbf{U})}{\partial y} = \frac{1}{Re}\left(\frac{\partial \mathbf{H}(\mathbf{U})}{\partial x} + \frac{\partial \mathbf{T}(\mathbf{U})}{\partial y}\right), \quad (6)$$

and a chemical kinetics part:

$$\frac{\partial \mathbf{U}}{\partial t} = \mathbf{S}(\mathbf{U}). \quad (7)$$

This splitting allows us to use a specific numerical scheme developed for the fluid dynamic part in conjunction with a numerical method especially developed to deal with stiff systems of ODEs for the chemical kinetics part. For Equation (6), we use the fifth-order weighted essentially non-oscillatory (WENO) scheme (Shu and Osher 1988, 1989; Jiang and Shu 1996) for the inviscid flux terms and the fourth-order central difference scheme (Shen, Zha, and Chen 2009; Shen, Wang, and Zha 2010) for the viscous flux terms. The third-order Runge–Kutta method is used to evolve the solution in time. The chemical kinetics part, Equation (7), is solved using CHEMEQ, a solver of stiff nonlinear ODEs, developed by Young et al. (Young and Boris 1977; Young 1980). For the boundaries we use Navier–Stokes characteristic boundary conditions (Poinsot and Lelef 1992; Poinsot and Veynate 2005).

3. Model reduction methodology

Projection-based methods derive a reduced-order model by projecting the governing equations onto a subspace spanned by a set of basis vectors (Antoulas, Sorensen, and Gugercin 2001). In this section, we describe the projection-based model reduction idea, the POD technique, and the DEIM employed in the approximation of the nonlinear source term.

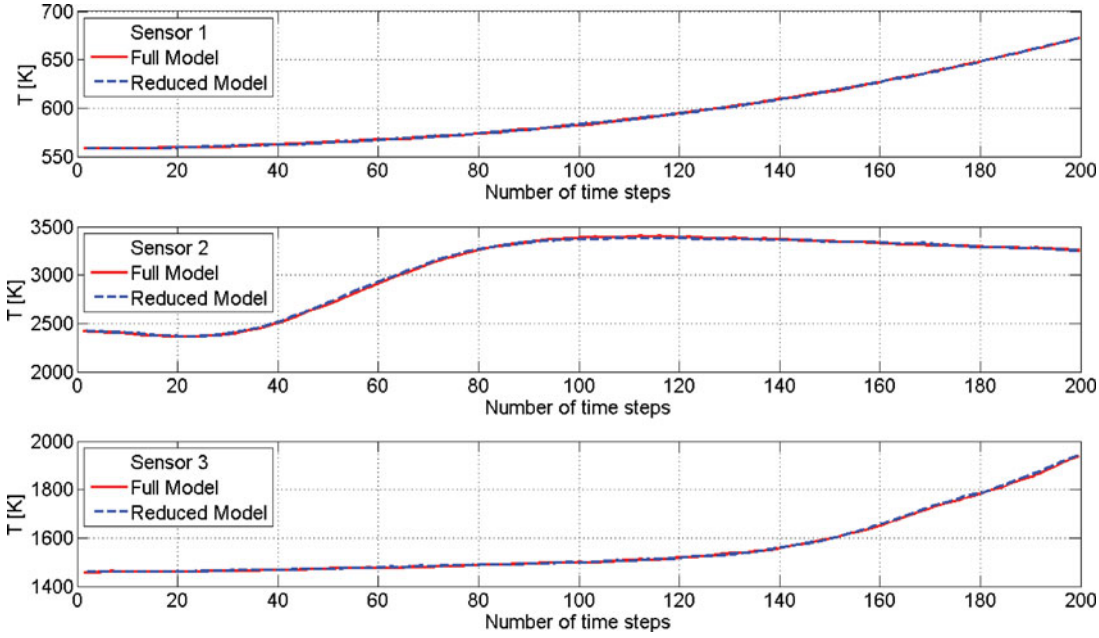

Figure 5. Comparison of solutions of the temperature evolution at three sensor locations between the POD–DEIM reduced model of size $K = 40$, $L = 60$ and the full model of size $M = 91,809$.

3.1. *Projection framework*

Consider the following nonlinear system of ODEs resulting from spatial discretisation of Equation (7):

$$\frac{d\mathbf{Y}}{dt} = \mathbf{g}(\mathbf{Y}, T, p) \tag{8}$$

with initial conditions $\mathbf{Y}(t = 0) = \mathbf{Y}^0$. Here, $\mathbf{Y} = \left[Y_1^1, \ldots, Y_1^N, \ldots, Y_{N_s}^1, \ldots, Y_{N_s}^N\right]^T \in \mathbb{R}^M$ is the vector of species mass fractions discretised over the computational domain, which has N grid points, T is the temperature of the mixture, and p is the pressure of the mixture.

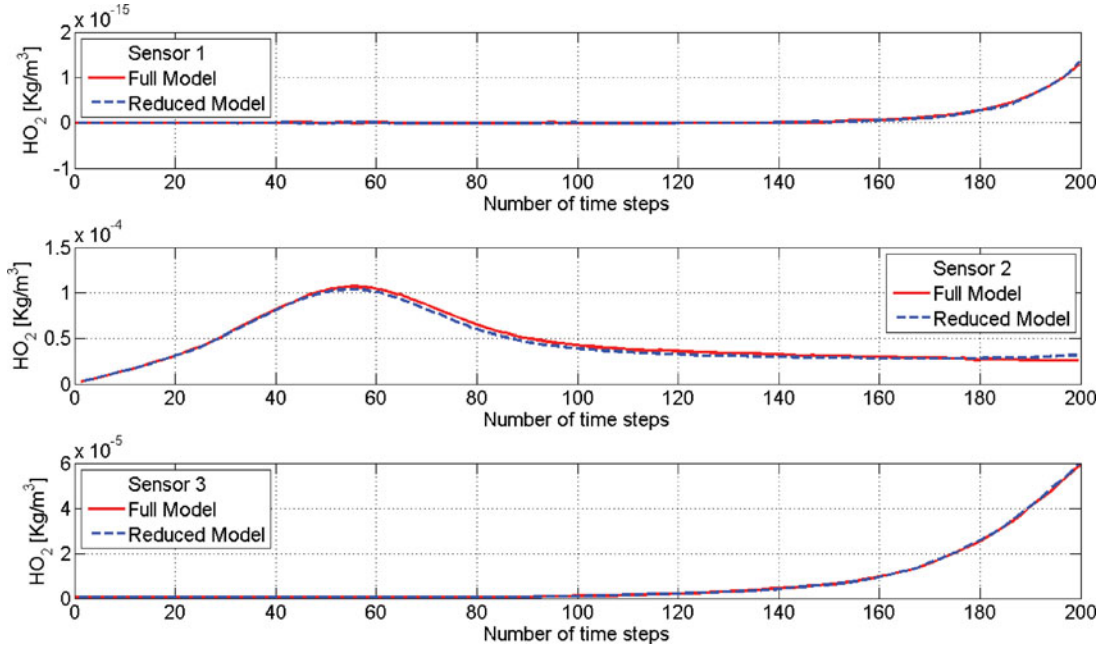

Figure 6. Comparison of solutions of the flame (HO_2) evolution at three sensor locations between the POD–DEIM reduced model of size $K = 40$, $L = 60$ and the full model of size $M = 91,809$.

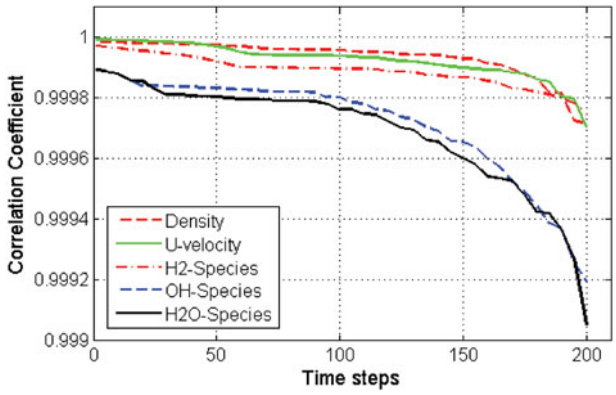

Figure 7. Correlation coefficients for the POD–DEIM reduced model of size $K = 40$, $L = 60$.

The vector $\mathbf{g}(\mathbf{Y}, T, p) = \left[g_1^1(\mathbf{Y}, T, p), \ldots, g_1^N(\mathbf{Y}, T, p), \ldots, g_{N_s}^1(\mathbf{Y}, T, p), \ldots, g_{N_s}^N(\mathbf{Y}, T, p)\right]^T \in \mathbb{R}^M$ contains the reaction rates over the computational domain. The total number of unknowns in (8) is $M = N_s N$, which becomes large as the number of chemical species and/or grid points is increased.

A reduced-order model for the system of equations (8) is derived by assuming that the state vector $\mathbf{Y}$ can be represented as a linear combination of K basis vectors,

$$\mathbf{Y} \approx \mathbf{V}\mathbf{Y}_r, \tag{9}$$

where $\mathbf{Y}_r \in \mathbb{R}^K$ is the reduced-state vector with $K \ll M$ and the matrix $\mathbf{V} \in \mathbb{R}^{M \times K}$ contains as columns orthonormal basis vectors v_i, $i = 1, \ldots, K$. Using Equation (9), the reduced-order model is obtained by performing Galerkin projection of the system of ODEs (8) onto the subspace spanned by the column basis vectors v_i,

$$\frac{d\mathbf{Y}_r(t)}{dt} = \mathbf{V}^T \mathbf{g}(\mathbf{V}\mathbf{Y}_r(t), T, p), \tag{10}$$

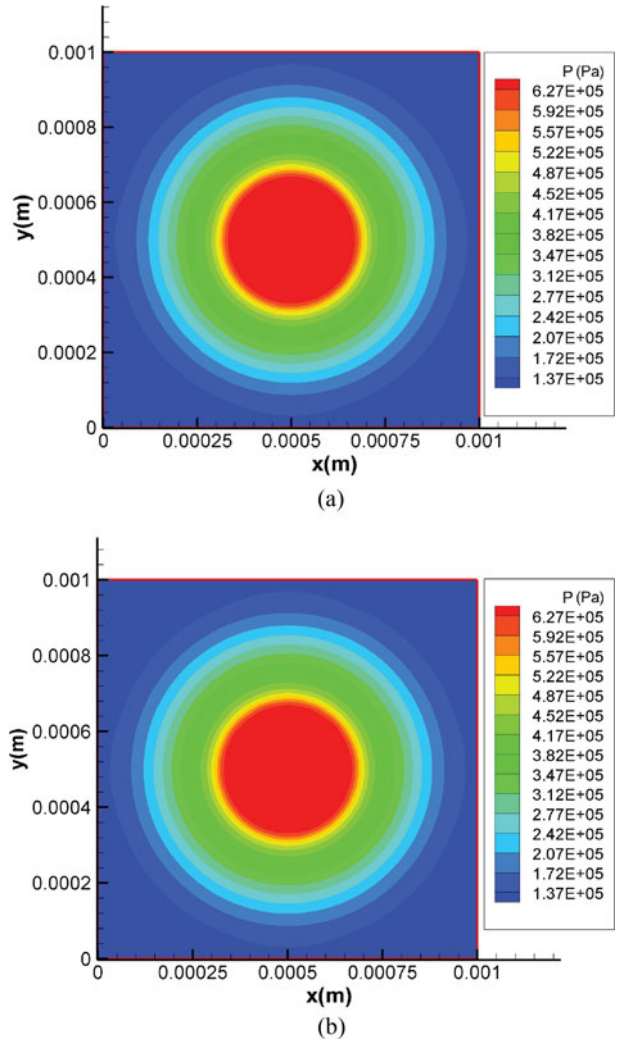

Figure 8. Comparison of the contours of pressure at time $t = 15\ \mu$s. (a) Full model of dimension $M = 91,809$. (b) POD–DEIM reduced model of dimension $K = 40$, $L = 40$.

Table 2. Average relative error and online computational time for different numbers of POD basis vectors (K). Computational times are normalised by the time of a full model chemistry time step.

POD			POD–DEIM			
K	Average relative error	Online time	K	L	Average relative error	Online time
1	1.33×10^{-1}	4.61×10^{-1}	1	40	2.36×10^{-1}	2.32×10^{-3}
5	3.27×10^{-2}	4.65×10^{-1}	5	40	6.11×10^{-2}	2.55×10^{-3}
10	5.01×10^{-3}	4.71×10^{-1}	10	40	2.47×10^{-2}	2.71×10^{-3}
20	1.16×10^{-3}	4.73×10^{-1}	20	40	1.39×10^{-3}	2.97×10^{-3}
40	3.18×10^{-4}	5.02×10^{-1}	40	40	8.65×10^{-4}	3.35×10^{-3}
60	1.11×10^{-4}	5.31×10^{-1}	60	40	5.95×10^{-4}	3.87×10^{-3}
80	4.59×10^{-5}	6.46×10^{-1}	80	40	4.78×10^{-4}	4.23×10^{-3}
100	8.47×10^{-6}	5.74×10^{-1}	100	40	4.28×10^{-4}	4.71×10^{-3}

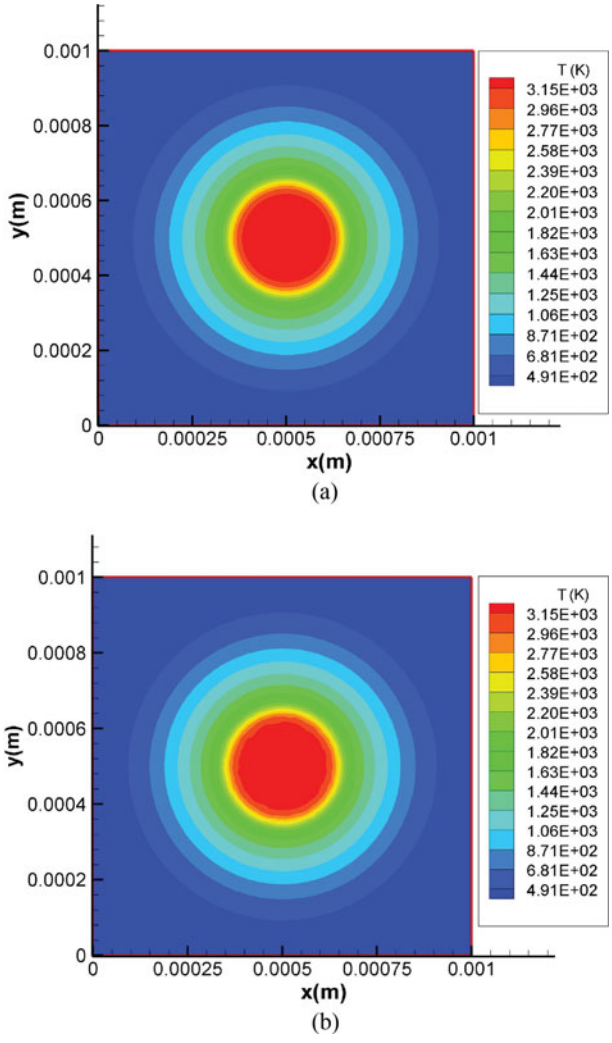

Figure 9. Comparison of the contours of temperature at time $t = 15\ \mu$s. (a) Full model of dimension $M = 91,809$. (b) POD–DEIM reduced model of dimension $K = 40$, $L = 40$.

with the initial condition $\mathbf{Y}_r^0 = \mathbf{V}^T\mathbf{Y}^0$. The choice of the basis vectors clearly affects the accuracy of the approximation. The K basis vectors can be obtained by many different methods. In this study, the basis vectors are constructed using the POD method of snapshots (Sirovich 1987).

Although the reduced-order model obtained after applying the projection technique is low in dimension, as can be observed in Equation (10), the evaluation of the nonlinear reaction source term at each time step still depends on the dimension M. This makes the solution of the obtained reduced-order model as expensive as the solution of the original system. An effective way to overcome this difficulty is to approximate the nonlinear function by projection and interpolation. This is the idea behind the DEIM (Chaturantabut and Sorensen 2010), which is a discrete version of the EIM proposed by Barrault et al. (2004), described in more detail later.

3.2. *Proper orthogonal decomposition*

The POD technique, also known as the Karhunen–Loève decomposition (Loève 1977), is a method for constructing basis vectors with global support that capture the dominant characteristics of a dynamical system. In the method of snapshots, such basis vectors (POD modes) are computed from an ensemble of solutions (snapshots) obtained by solving the large-scale system for selected values of parameters and inputs. The POD modes are computed as follows.

Given a set of Q snapshots $\{\mathbf{Y}_j\}_{j=1}^{Q}$, where $\mathbf{Y}_j \in \mathbb{R}^M$, the POD computes the set of $K \leq Q$ basis vectors $\{\mathbf{v}_i\}_{i=1}^{K}$, where $\mathbf{v}_i \in \mathbb{R}^M$ is the ith basis vector, as the set that solves the minimisation problem

$$\min_{\{\mathbf{v}\}_{i=1}^{K}} \sum_{j=1}^{Q} \| \mathbf{Y}_j - \sum_{i=1}^{K} (\mathbf{Y}_j^T\mathbf{v}_i)\mathbf{v}_i \|_2^2, \quad \text{s.t. } \mathbf{v}_i^T\mathbf{v}_j = \delta_{ij}, \ 1 \leq i, j \leq K. \tag{11}$$

The solution of Equation (11) can be obtained by finding the singular vectors of the snapshot matrix $\mathbf{Y} = [\mathbf{Y}_1, \ldots, \mathbf{Y}_Q] \in \mathbb{R}^{M\times Q}$. In particular, supposing that the singular value decomposition of $\mathbf{Y}$ is

$$\mathbf{Y} = \mathbf{V}\Sigma\mathbf{W}^T, \tag{12}$$

where $\mathbf{V} = [\mathbf{v}_1, \ldots, \mathbf{v}_Q] \in \mathbb{R}^{M\times Q}$ and $\mathbf{W} = [\mathbf{w}_1, \ldots, \mathbf{w}_Q] \in \mathbb{R}^{M\times Q}$ are orthogonal and the singular values are $\mathbf{\Sigma} = \text{diag}(\sigma_1, \ldots, \sigma_Q) \in \mathbb{R}^{Q\times Q}$ with $\sigma_1 \geq \sigma_2 \geq \cdots \geq \sigma_Q > 0$, then the POD basis is $\{\mathbf{v}\}_{i=1}^{K} \subset \mathbf{V} \in \mathbb{R}^{M\times Q}$. The POD gives the optimal representation, in the least-squares sense, of the set of snapshots Q. The error in approximating the snapshots using K POD modes is given by

$$\sum_{j=1}^{Q} \| \mathbf{Y}_j - \sum_{i=1}^{K} (\mathbf{Y}_j^T\mathbf{v}_i)\mathbf{v}_i \|_2^2 = \sum_{i=K+1}^{Q} \sigma_i^2. \tag{13}$$

3.3. *Discrete empirical interpolation method*

The DEIM provides an efficient approach to build reduced-order models whose computational cost is independent of the dimension of the original large-scale system. To construct the POD–DEIM reduced-order model, two sets of basis vectors are used: the POD modes $\mathbf{V}$ obtained from the solution snapshots and the DEIM modes $\mathbf{U}$ obtained from snapshots of the nonlinear source term. Computation of $\mathbf{U}$ proceeds as described above for $\mathbf{V}$, but replacing state snapshots $\mathbf{Y}_j \equiv \mathbf{Y}(t_j, T, p)$ with snapshots of the nonlinear terms $\mathbf{g}_j \equiv \mathbf{g}(\mathbf{Y}_j, T, p)$. The nonlinear source term is

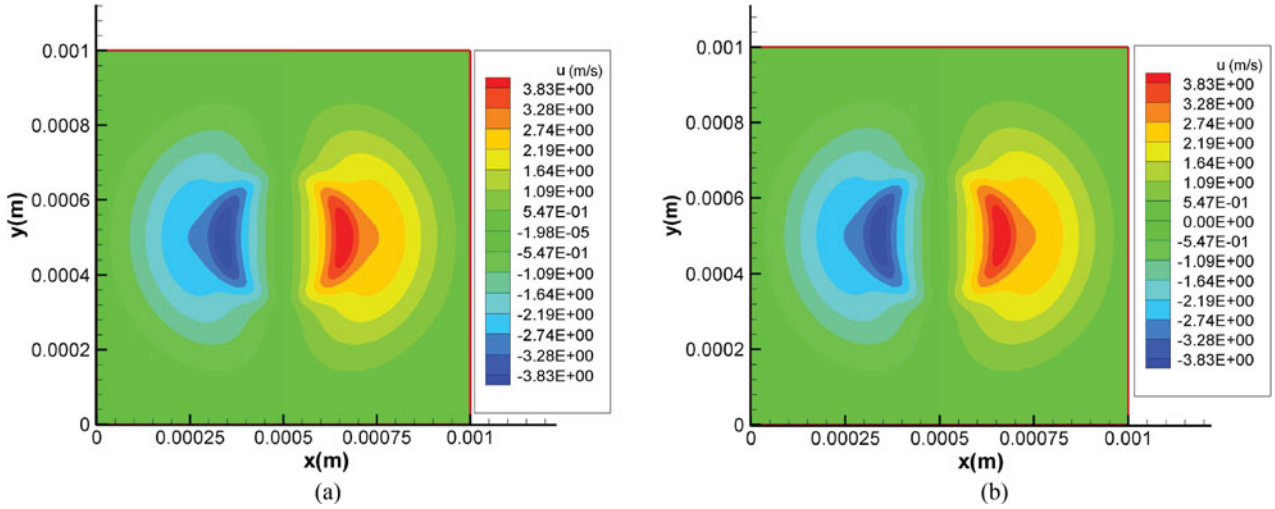

Figure 10. Comparison of the contours of u-velocity component at time t=15 μs. (a) Full model of dimension $M = 91,809$. (b) POD–DEIM reduced model of dimension $K = 40$, $L = 40$.

then approximated by a linear combination of L basis vectors $\mathbf{U} \in \mathbb{R}^{M\times L}$ with corresponding expansion coefficients $\mathbf{c} \in \mathbb{R}^{L}$ as

$$\mathbf{g}(\mathbf{Y}, T, p, t) \approx \mathbf{U}\mathbf{c}(t). \tag{14}$$

From the DEIM basis vectors $\mathbf{U}$, the DEIM finds a set of interpolation indices that allow the determination of the coefficients $\mathbf{c}$ in (14). This involves the evaluation of the nonlinear source term at only a subset of points $L \ll M$, hence eliminating the dependence on M of the reduced-order model. The POD–DEIM reduced-order model then becomes

$$\frac{d\mathbf{Y}_r(t)}{dt} = \mathbf{V}^T\mathbf{U}(\mathbf{P}^T\mathbf{U})^{-1}\mathbf{g}(\mathbf{P}^T\mathbf{V}\mathbf{Y}_r(t), T, p), \tag{15}$$

where $\mathbf{P} \in \mathbb{R}^{M\times L}$ is a matrix defining the interpolation indices (defined in more detail below).

In this study, we use the DEIM algorithm proposed in Chaturantabut and Sorensen (2010) since it provides an efficient methodology to compute the desired interpolation indices for determining the coefficients $\mathbf{c}(t)$. The algorithm is shown in Table 1.

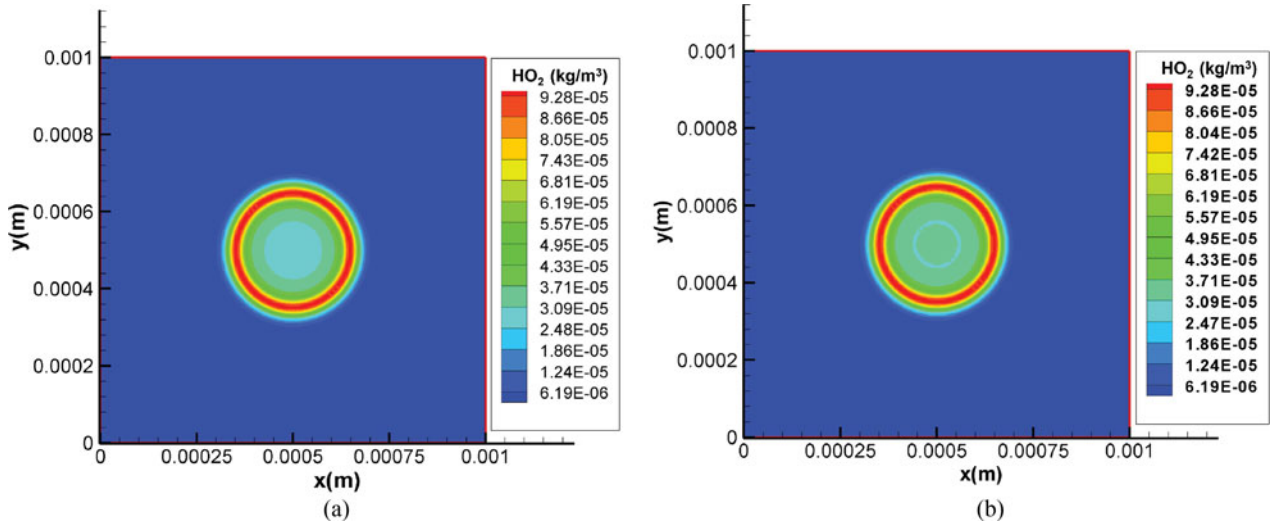

Figure 11. Comparison of the contours of concentration of species HO_2 at time $t = 15$ μs. (a) Full model of dimension $M = 91,809$. (b) POD–DEIM reduced model of dimension $K = 40$, $L = 40$.

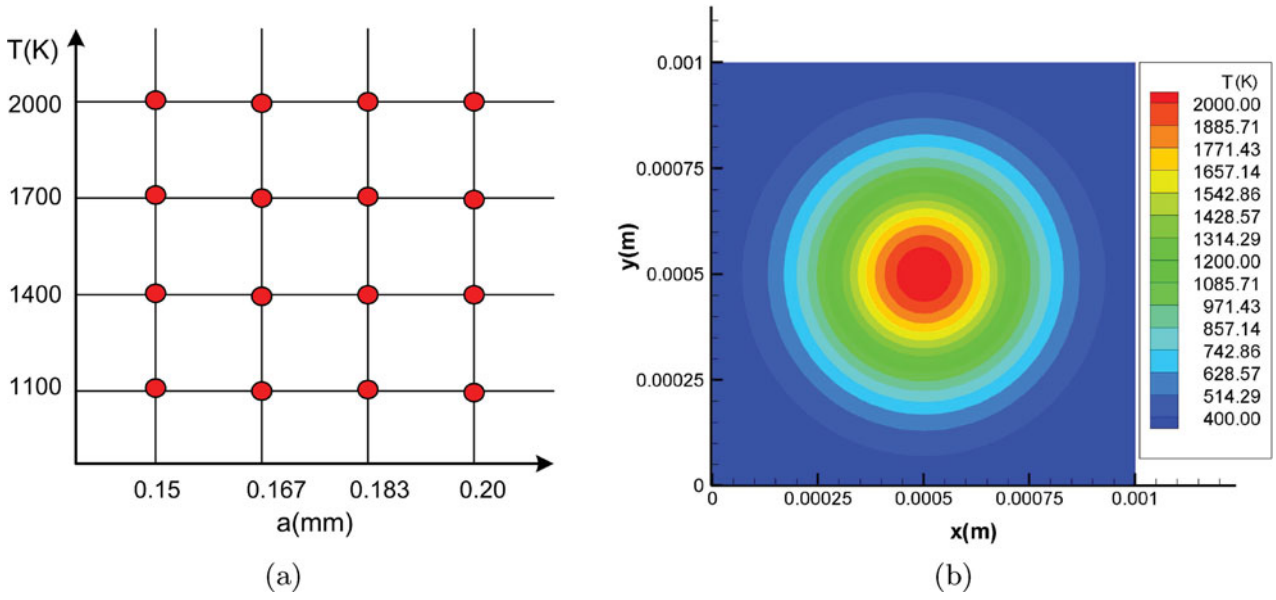

Figure 12. Input parameters: (a) 16 sample points. (b) Gaussian distribution of temperature for a typical case ($T_0 = 2000$ K and $a = 0.2$ mm).

In the algorithm, $\max\{|\cdot|\}$ implies finding the index of the maximum absolute value of $\cdot$, and $\{p_1, \ldots, p_L\}$ are the desired L interpolation indices, $\mathbf{P} = [\mathbf{e}_{p_1}, \ldots, \mathbf{e}_{p_L}]$, where $\mathbf{e}_{p_i} = [0, \ldots, 0, 1, 0, \ldots, 0]^T \in \mathbb{R}^M$ is column p_i of the identity matrix $\mathbf{I} \in \mathbb{R}^{M\times M}$ for $i = 1, \ldots, L$.

Once the indices are determined and the matrix $\mathbf{P}$ is built, the expansion coefficients are computed as

$$\mathbf{c}(t) = (\mathbf{P}^T\mathbf{U})^{-1}\mathbf{P}^T\mathbf{g}(\mathbf{Y}, T, p, t). \tag{16}$$

By substituting (16) in Equation (14), we obtain

$$\mathbf{g}(\mathbf{Y}, T, p, t) \approx \mathbf{U}(\mathbf{P}^T\mathbf{U})^{-1}\mathbf{g}(\mathbf{P}^T\mathbf{Y}, T, p, t). \tag{17}$$

Since in our case the nonlinear reaction source term can be evaluated componentwise at its input vector, Equation (17) becomes

$$\mathbf{g}(\mathbf{Y}_r, T, p, t) \approx \mathbf{V}^T\mathbf{U}(\mathbf{P}^T\mathbf{U})^{-1}\mathbf{g}(\mathbf{P}^T\mathbf{V}\mathbf{Y}_r, T, p, t), \tag{18}$$

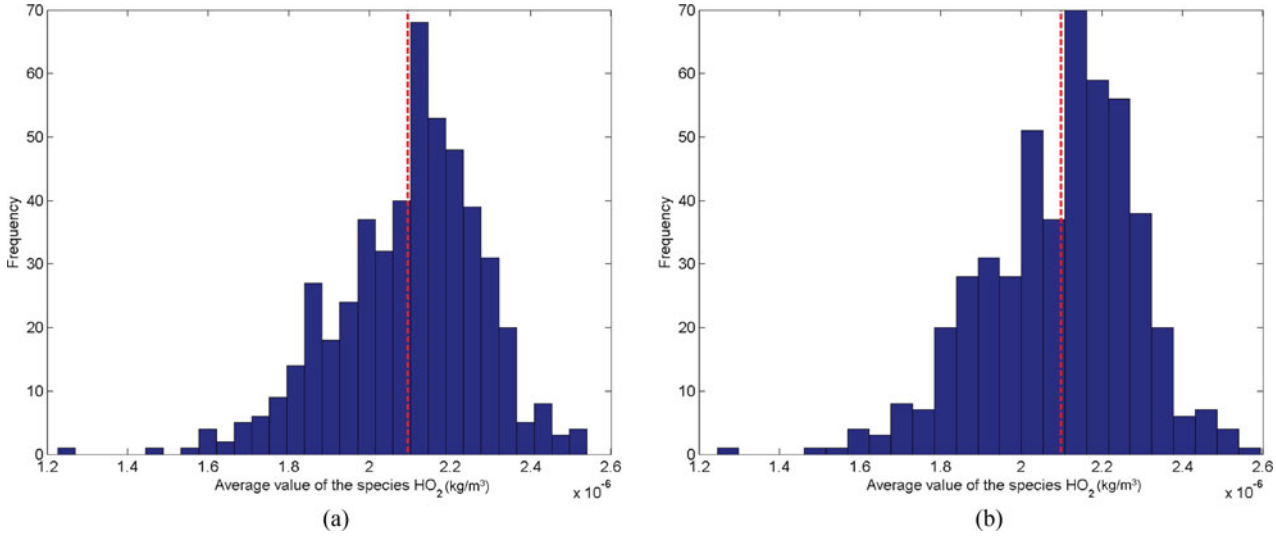

Figure 13. Comparison of histograms of average concentration of species HO_2 between the full model and reduced-order model. MCS results are shown for 500 randomly sampled values of the peak temperature of the initial condition. The dashed line shows the sample mean. (a) Full model. (b) Reduced model.

where the temperature and pressure are evaluated at interpolation points. Equation (18) is the DEIM approximation of the nonlinear source term. The terms $\mathbf{V}^T\mathbf{U}(\mathbf{P}^T\mathbf{U})^{-1} \in \mathbb{R}^{K\times L}$ and $\mathbf{P}^T\mathbf{V} \in \mathbb{R}^L$ can be precomputed in an offline stage. Therefore, the online computation of the reduced-order model requires only the solution of a system of K nonlinear equations with just L evaluations of $\mathbf{g}(., T, p)$ and the temperature and pressure also evaluated at the L interpolation points.

4. A POD–DEIM reduced-order model for a Gaussian premixed flame

In this section, we present the result of POD–DEIM model reduction for a multistep chemical reacting flow problem of a Gaussian premixed flame.

4.1. Problem setup

The evolution of the Gaussian flame is modelled by the system of coupled nonlinear PDEs introduced in Section 2. The gas mixture is composed of 9 chemical species (O_2, H_2, O, H, OH, HO_2, H_2O_2, H_2O, Ar) participating in 19 reversible elementary reactions corresponding to the chemical kinetics model employed in Wilson and MacCormack (1990). The transport properties of the mixture and the species are computed using classical kinetic theory and the mixture-average approach, and employing the GRI-Mech 3.1 database (Smith et al., n.d.). Whenever third-body reactions appear in the kinetic mechanism, the third-body factors are $\alpha_{ki} = 2.5$ for H_2, $\alpha_{ki} = 16.0$ for H_2O, and $\alpha_{ki} = 1.0$ otherwise. The POD–DEIM model reduction technique is applied to the nonlinear source term (7), since, as in typical reacting flow applications, the solution of this term drives the computational cost of the numerical simulation.

For all simulations, a two-dimensional square domain of 1.0 mm $\times$ 1.0 mm is discretised using a uniform mesh grid with 101 grid points in each direction. Figure 1(a) shows the computational grid. The dimension of the full-model unknowns $\mathbf{Y}$ is $M = 91,809$. Initial conditions specify a pressure of 101,325.0 Pa and velocity components of 0 m/s. A premixed mixture of $H_2/O_2/Ar$ with mole fractions 0.333: 0.167: 0.5 is imposed at each grid point of the computational domain. To start the reaction (the flame), we use a two-dimensional Gaussian distribution located at the centre of the domain (see Figure 1(b)),

$$T(x, y) = T_0 e^{-\left(\frac{(x-x_0)^2}{2a^2} + \frac{(y-y_0)^2}{2a^2}\right)}, \qquad (19)$$

where T_0 is the temperature amplitude, a is the width of the temperature distribution, and (x_0, y_0) are the coordinates of the centre point. Outlet subsonic flow characteristic boundary conditions (Lodato, Domingo, and Vervisch 2008) are applied to the four boundaries of the domain (see Figure 1(a)).

4.2. Fixed parameters and inputs

We first test the capabilities of the reduced-order model in terms of the approximation errors and computational time savings. To this end, several models of different sizes (values of K and L) are constructed for fixed simulation parameters and inputs. All the models are built using 400 snapshots of state solution $\mathbf{Y}$ and 400 corresponding snapshots of nonlinear term $\mathbf{g}(\mathbf{Y}, T, p)$. For each model, the snapshots are collected from simulations of the full-order model lasting 200 flow time steps. To assess the performance of the reduced-order models, a simulation of 200 flow time steps is carried out for each reduced model and the average relative error at the final time step and the average simulation time of one chemistry time step are calculated.

Figure 2 shows the average relative error of the solutions obtained using the reduced models of different sizes. The results indicate that both the number of POD modes and the number of interpolation points drive the average relative error when the number of POD modes is smaller than 40. For reduced-order models with state dimensions greater than 40, the average relative error is driven by the number of interpolation points, indicating that the approximation of the nonlinear term is the most significant source of error.

Figure 3 shows comparisons of the average computational time for one chemistry time step between the full model, classical POD reduced-order models, and POD–DEIM reduced-order models, again for different choices of K and L. Figure 3 shows that the computational time is driven by both K and L. It also shows that POD–DEIM models are on average two orders of magnitude faster than POD models. However, if we consider models of similar size (for example, a POD model of size $K = 40$ and a POD–DEIM model of size $K = 40$, $L = 60$), the POD model is more accurate (as shown in Figure 2). We also note that despite the good speedup factors obtained by the POD–DEIM models (of order 100) in the solution of the nonlinear source term, the speedup factor for the coupled flow-chemistry simulation is of the order of a factor of 10. The reason for this is that the fluid dynamics part in the operator-splitting scheme is still solved in full dimension. POD–DEIM reduced-order models for the Navier–Stokes equations could also be derived (Stefanescu and Navon 2013; Xiao et al. 2014) and used, which would lead to overall greater speed-up.

Figures 4–6 compare the time evolution of the outputs of interest – pressure, temperature, and HO_2 concentration – at three sensor locations: $(x; y) = (0.15; 0.15)$, $(0.5; 0.25)$, and $(0.5; 0.5)$, between the full model of size $M = 91,809$ and POD–DEIM reduced-order model of size $K = 40$, $L = 60$. The results show that the reduced model can accurately approximate the solution of the full model even for the most sensitive quantity in this simulation,

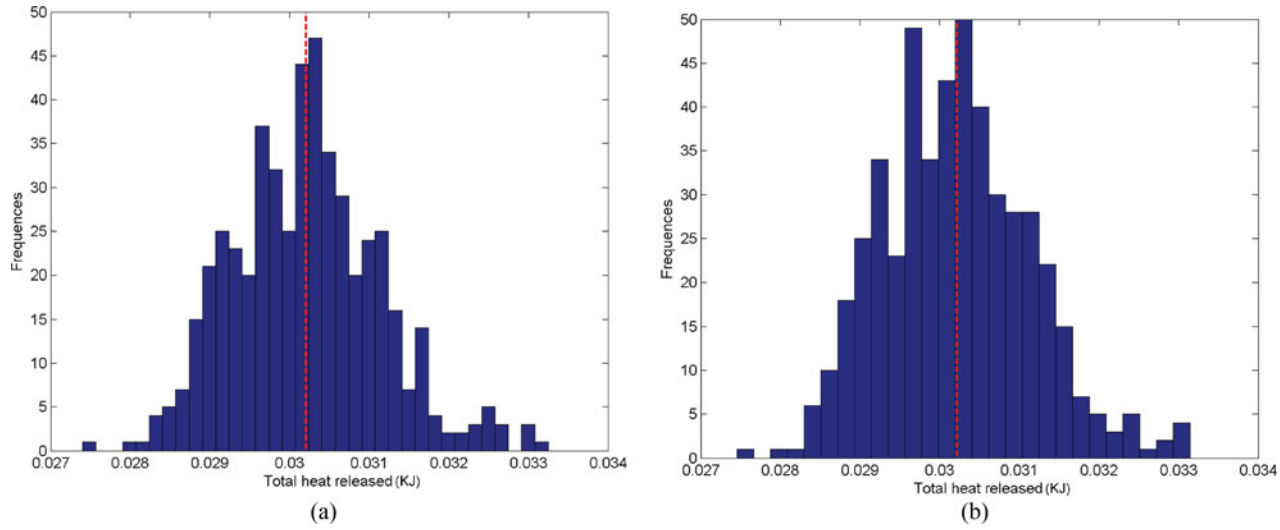

Figure 14. Comparison of histograms of total heat released between the full model and reduced-order model. MCS results are shown for 500 randomly sampled values of the peak temperature of the initial condition. The dashed line shows the sample mean. (a) Full model. (b) Reduced model.

concentration of species HO_2, as shown in Figure 6. We further verify the quality of the reduced models by calculating the Pearson correlation coefficients between the full and the POD–DEIM reduced-order models for each state quantity, following Stefanescu and Navon (2013). Figure 7 shows the Pearson correlation coefficient for some relevant state variables for the POD–DEIM reduced model of size $K = 40$, $L = 60$. The coefficients vary between 0.99999 and 0.999, showing that the reduced model is highly correlated with the full model throughout the entire simulated time.

Table 3. Comparison between the full model and reduced-order model. MCS results are shown for the average value of species HO_2 and total heat released for 500 randomly sampled values of the peak temperature of the initial conditions.

Name	Full model	Reduced model
Model size	91809	60
Offline cost	–	16.65 h
Online cost	464.87 h	45.83 h
Mean of total heat released	3.02×10^{-2}	3.02×10^{-2}
Variance of total heat released	8.51×10^{-7}	8.85×10^{-7}
Mean of species HO_2	2.10×10^{-6}	2.10×10^{-6}
Variance of species HO_2	3.34×10^{-14}	3.53×10^{-14}

4.3. *Varying Prandtl number: Pr ∈ [0.5, 1.0]*

In combustion processes, the Prandtl number, Pr, plays an important role in heat convection and diffusion. In this section, we test the ability of a POD–DEIM reduced-order model to estimate solutions of the full model for values of Pr in the range [0.5, 1.0]. The reduced-order model is constructed using 400 snapshots, which are taken from two simulations of the full system at $Pr = 0.5$ and $Pr = 1.0$. Two hundred snapshots, one at every flow time step, are taken for each value of Pr. To demonstrate the prediction capability of our reduced-order model, we select a value of $Pr = 0.8$ and simulate the full model, POD reduced-order models of varying dimension, and POD–DEIM reduced-order models of varying dimension K and fixed $L = 40$. Table 2 summarises the results obtained in terms of average relative error and relative computational simulation time, with respect to the full model, of one chemistry time step. It can be seen from the table that the POD models are, in general, more accurate but they are again about two orders of magnitude slower than the models constructed using POD–DEIM. In addition, the table shows that for a satisfactory level of accuracy, say, the average relative error of about 5.0×10^{-4}, the computation of the nonlinear source term using the POD–DEIM model is more than 200 times faster than the full model calculation. Figures 8–11 compare the solutions between the full model of dimension $M = 91,809$ and the POD–DEIM reduced-order model of dimension $K = 40$, $L = 40$ at $t = 15$ μs. The figures show that the model is able to predict accurately the solution for $Pr = 0.8$.

4.4. *Analysis of the impact of parameter variability on the total heat release and average concentration of HO_2*

The POD–DEIM reduced-order model is now used to analyse the impact on outputs of interest of variability in the parameters describing the initial Gaussian temperature profile given by Equation (19). To this end, a POD–DEIM model is

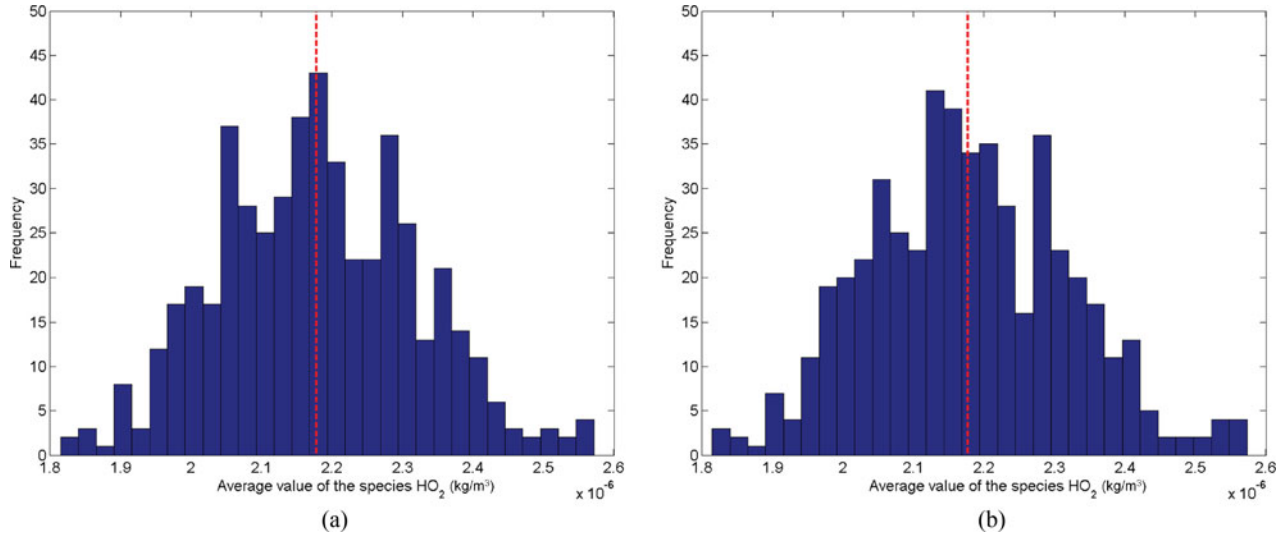

Figure 15. Comparison of histograms of average concentration of species HO_2 between the full model and reduced-order model. MCS results are shown for 500 randomly sampled values of the initial condition width. The dashed line shows the sample mean. (a) Full model. (b) Reduced model.

constructed using 4000 snapshots. The snapshots are computed from 16 simulations corresponding to the combination of four different values of the temperature amplitude T_0 with four different values of the width a of the Gaussian temperature profile (see Figure 12(a)). For each of the simulations, 250 snapshots are taken corresponding to 250 flow time steps. The range of amplitude of temperature is chosen so that the chemical reactions occur slowly at the minimum value of the amplitude and quickly at its maximum value. For the width, the range is chosen to ensure that the boundary conditions are satisfied for its maximum value. A particular case of the initial condition is shown in Figure 12(b).

Monte Carlo simulations (MCSs) are then performed for two cases in order to analyse the impact of variability in amplitude and width on the total heat release and on the average concentration of species HO_2 over the computational domain. In the first case, the width is kept constant at $a = 0.183$. The amplitude T_0 is modelled as a Gaussian random variable with a mean of 1550 K and standard deviation of 26 K. 500 samples are drawn randomly from this normal distribution. In the second case, the width is modelled as

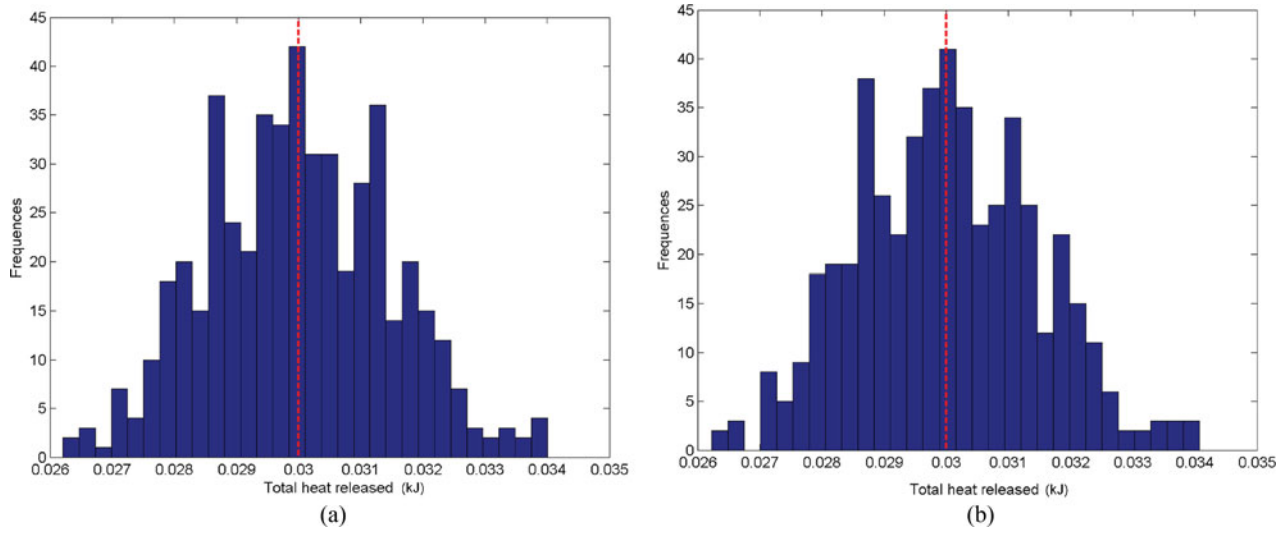

Figure 16. Comparison of histograms of total heat released between the full model and reduced-order model. MCS results are shown for 500 randomly sampled values of the initial condition width. The dashed line shows the sample mean. (a) Full model. (b) Reduced model.

Table 4. Comparison between the full model and reduced-order model. MCS results are shown for the average value of species HO_2 and total heat released for 500 randomly sampled values of the initial condition width.

Name	Full model	Reduced model
Model size	91, 809	60
Offline cost	–	16.65 h
Online cost	442.37 h	45.83 h
Mean of total heat released	3.00×10^{-2}	3.00×10^{-2}
Variance of total heat released	2.12×10^{-6}	2.11×10^{-6}
Mean of species HO_2	2.18×10^{-6}	2.18×10^{-6}
Variance of species HO_2	2.00×10^{-14}	2.02×10^{-14}

a Gaussian random variable with a mean of 0.175 mm and standard deviation of 4.5×10^{-3} mm. The amplitude is kept constant at $T_0 = 1700$ K. Again, 500 random samples are used in the MCS. In both cases, the samples are evaluated using the full model and a POD–DEIM reduced model of order $K = 60$, $L = 60$.

Figures 13 and 14 show the comparison between the full and reduced model histograms for the average concentration of species HO_2 and the total heat release, for the first case with varying T_0. Table 3 summarises estimated statistics and computation times. The results show that the reduced model is able to estimate the mean and the variance of the total heat release and of the average concentration of HO_2 with small errors. In fact, the mean estimates of the reduced-order model agree with those of the full model to within two decimal places.

Figures 15 and 16 show the comparison between the full and reduced model histograms for the average concentration of species HO_2 and the total heat release, for the second case with varying width a. Table 4 summarises estimated statistics and computation times. The reduced model again estimates the mean and the variance of the total heat released and species HO_2 accurately.

5. Conclusions

The contribution of this paper is to show how projection-based reduced modelling using the POD method combined with the DEIM is an effective strategy for reducing the cost of chemical kinetics evaluations in reacting flow simulations. The reduced-order models can be parameterised and then used for design space studies as well as quantification of the effects of parameter uncertainties on output quantities of interest. The methodology was demonstrated here using a premixed H_2/O_2/Ar mixture problem, but is applicable to general reaction models. Here we focused on application of the POD–DEIM approach to the chemical kinetics model only; however, the POD method can also be applied to obtain a reduced model of the fluid dynamics model to gain additional reduction in overall simulation time of the coupled system. An important area of future research is to extend the POD–DEIM approach to optimisation of systems governed by PDEs. While more challenging than the parameterised forward simulation problem considered here, PDE-constrained optimisation problems could benefit significantly in computational gains from efficient reduced modelling strategies.

Acknowledgements

This work was supported by the Singapore-MIT Alliance Computational Engineering Programme and by the Air Force Office of Scientific Research Computational Mathematics Program, Grant FA9550-12-1-0420, Program Manager F. Fahroo.

References

Amabili, M., A. Sarkar, and M. P. Païdoussis. 2006. "Chaotic Vibrations of Circular Cylindrical Shells: Galerkin Versus Reduced-Order Models Via the Proper Orthogonal Decomposition Method." *Journal of Sound and Vibration* 290(3–5): 736–762. doi: 10.1016/j.jsv.2005.04.034.

Antoulas, A., D. Sorensen, and S. Gugercin. 2001. *A Survey of Model Reduction Methods for Large-Scale Systems*. Providence, RI: American Mathematical Society.

Astrid, P., S. Weiland, K. Willcox, and T. Backx. 2008. "Missing Point Estimation in Models Described by Proper Orthogonal Decomposition." *IEEE Transactions on Automatic Control* 10: 2237–2251. doi: 10.1109/TAC.2008.2006102.

Barrault, M., Y. Maday, N. C. Nguyen, and A. Patera. 2004. "An 'Empirical Interpolation' Method: Application to Efficient Reduced-Basis Discretization of Partial Differential Equations." *Comptes Rendus Mathématique* 339(9): 667–672. doi: 10.1016/j.crma.2004.08.006.

Brown, N. J., G. Li, and M. L. Koszykowski. 1997. "Mechanism Reduction Via Principal Component Analysis." *International Journal of Chemical Kinetics* 29(6): 393–414. doi: 10.1002/(SICI)1097-4601(1997)29:6⟨393::AID-KIN1⟩3.0.CO;2-P.

Buffoni, M., S. Camarri, A. Iollo, and M. V. Salvetti. 2006. "Low-Dimensional Modelling of a Confined Three-Dimensional Wake Flow." *Journal of Fluid Mechanics* 569: 141–150. doi: 10.1017/S0022112006002989.

Chase, M. W. 1998. *NIST-JANAF Thermochemical Tables*. Gaithersburg, MD: National Institute of Standards and Technology.

Chaturantabut, S., and D. Sorensen. 2010. "Nonlinear Model Reduction Via Discrete Empirical Interpolation." *SIAM Journal on Scientific Computing* 32: 2737–2764.

Everson, R., and L. Sirovich. 1995. "The Karhunen-Loéve Procedure for Gappy Data." *Journal of the Optical Society of America* 12(8): 1657–1664. doi: 10.1364/JOSAA.12.001657.

Feldmann, P., and R. W. Freund. 1995. "Efficient Linear Circuit Analysis by Padé Approximation Via the Lanczos Process." *IEEE Transactions on Computer-Aided Design of Integrated Circuits and Systems* 14(5): 639–649. doi: 10.1109/43.384428.

Gallivan, K., E. Grimme, and P. Van Dooren. 1994. "Padé Approximation of Large-Scale Dynamic Systems with Lanczos Methods." In *Proceedings of the 33rd IEEE Conference on Decision and Control*, 443–448. New York: IEEE. doi: 10.1109/CDC.1994.410886.

Gallivan, K., E. Grimme, and P. Van Dooren. 1999. "Model Reduction of Large-Scale Systems: Rational Krylov Versus Balancing Techniques." In *Error Control and Adaptivity in Scientific Computing*, edited by Haydar Bulgak and Christoph Zenger, 177–190. Dordrecht: Springer.

Grepl, M. A., Y. Maday, N. C. Nguyen, and A. Patera. 2007. "Efficient Reduced-Basis Treatment of Nonaffine and Nonlinear Partial Differential Equations." *ESAIM: Mathematical Modelling and Numerical Analysis* 41(3): 575–605. doi: 10.1051/m2an:2007031.

Grimme, E. J. 1997. "Krylov Projection Methods for Model Reduction." PhD thesis, Coordinated Science Laboratory, University of Illinois at Urbana-Champaign.

Gugercin, S., and A. Antoulas. 2004. "A Survey of Model Reduction by Balanced Truncation and Some New Results." *International Journal of Control* 77(8): 748–766. doi: 10.1080/00207170410001713448.

Hadjinicolaou, M., and D. A. Goussis. 1999. "Asymptotic Solution of Stiff PDEs with the CSP Method: The Reaction Diffusion Equation." *SIAM Journal on Scientific Computing* 20: 781–810. doi: 10.1137/S1064827596303995.

Holmes, P., J. L. Lumley, and G. Berkooz. 1998. *Turbulence, Coherent Structures, Dynamical Systems and Symmetry*. Cambridge: Cambridge University Press.

Jiang, G.-S., and C.-W. Shu. 1996. "Efficient Implementation of Weighted ENO Schemes." *Journal of Computational Physics* 126(1): 202–228. doi: 10.1006/jcph.1996.0130.

Kerschen, G., J.-C. Golinval, A. F. Vakakis, and L. A. Bergman. 2005. "The Method of Proper Orthogonal Decomposition for Dynamical Characterization and Order Reduction of Mechanical Systems: An Overview." *Nonlinear Dynamics* 41: 147–169. doi: 10.1007/s11071-005-2803-2.

Lam, S. H. 1993. "Using CSP to Understand Complex Chemical Kinetics." *Combustion Science and Technology* 89: 375–404. doi: 10.1080/00102209308924120.

Lam, S. H., and D. A. Goussis. 1994. "The CSP Method for Simplifying Kinetics." *International Journal of Chemical Kinetics* 26(4): 461–486. doi: 10.1002/kin.550260408.

Lodato, G., P. Domingo, and L. Vervisch. 2008. "Three-Dimensional Boundary Conditions for Direct and Large-Eddy Simulation of Compressible Viscous Flows." *Journal of Computational Physics* 227(10): 5105–5143. doi: 10.1016/j.jcp.2008.01.038.

Loève, M. 1977. *Probability Theory I–II*. New York: Springer-Verlag.

Lucia, D. J., P. I. King, and P. S. Beran. 2003. "Reduced Order Modeling of a Two-Dimensional Flow with Moving Shocks." *Computers and Fluids* 32: 917–938. doi: 10.1016/S0045-7930(02)00035-X.

Ma, X., and G. E. Karniadakis. 2002. "A Low-Dimensional Model for Simulating Three-Dimensional Cylinder Flow." *Journal of Fluid Mechanics* 458: 181–190. doi: 10.1017/S0022112002007991.

Maas, U., and S. B. Pope. 1992a. "Implementation of Simplified Chemical Kinetics Based on Intrinsic Low-Dimensional Manifolds." *Symposium (International) on Combustion* 24(1): 103–112. doi: 10.1016/S0082-0784(06)80017-2.

Maas, U., and S. B. Pope. 1992b. "Simplifying Chemical Kinetics: Intrinsic Low Dimensional Manifolds in Composition Space." *Combustion and Flame* 88: 239–264. doi: 10.1016/0010-2180(92)90034-M.

Maas, U., and S. B. Pope. 1994. "Laminar Flame Calculations Using Simplified Chemical Kinetics Based on Intrinsic Low-Dimensional Manifolds." *Symposium (International) on Combustion* 25(1): 1349–1356. doi: 10.1016/S0082-0784(06)80777-0.

McBride, B. J., and G. Sanford. 1994. *Computer Program for Calculation of Complex Chemical Equilibrium Compositions and Applications I. Analysis* (NASA report RP-1311). Cleveland, OH: NASA Glenn (formerly Lewis) Research Center.

McBride, B. J., and G. Sanford. 1996. *Computer Program for Calculation of Complex Chemical Equilibrium Compositions and Applications II. User's Manual and Program Description* (NASA report RP-1311-p2). Cleveland, OH: NASA Glenn (formerly Lewis) Research Center.

Peters, N., and F. A. Williams. 1987. "The Asymptotic Structure of Stoichiometric Methane-Air Flames." *Combustion and Flame* 68(2): 185–207. doi: 10.1016/0010-2180(87)90057-5.

Poinsot, T., and S. K. Lelef. 1992. "Boundary Conditions for Direct Simulations of Compressible Viscous Flows." *Journal of Computational Physics* 101(1): 104–129. doi: 10.1016/0021-9991(92)90046-2.

Poinsot, T., and D. Veynante. 2005. *Theoretical and Numerical Combustion*. 2nd ed. R.T. Edwards.

Ramshaw, J. D. 1980. "Partial Chemical Equilibrium in Fluid Dynamics." *Physics of Fluids* 23(4): 675–680. doi: 10.1063/1.863052.

Shen, Y., B. Wang, and G. Zha. 2010. "Implicit WENO Scheme and High Order Viscous Formulas for Compressible Flows." In *Proceedings of the 25th AIAA Applied Aerodynamics Conference*. Miami, FL. doi: 10.2514/6.2007-4431.

Shen, Y., G. Zha, and X. Chen. 2009. "High Order Conservative Differencing for Viscous Terms and the Application to Vortex-Induced Vibration Flows." *Journal of Computational Physics* 228(22): 8283–8300. doi: 10.1016/j.jcp.2009.08.004.

Shu, C.-W., and S. Osher. 1988. "Efficient Implementation of Essentially Non-Oscillatory Shock-Capturing Schemes." *Journal of Computational Physics* 77(2): 439–471. doi: 10.1016/0021-9991(88)90177-5.

Shu, C.-W., and S. Osher. 1989. "Efficient Implementation of Essentially Non-Oscillatory Shock-Capturing Schemes II." *Journal of Computational Physics* 83(1): 32–78. doi: 10.1016/0021-9991(89)90222-2.

Sirovich, L. 1987. "Turbulence and the Dynamics of Coherent Structures. I – Coherent Structures. II – Symmetries and Transformations. III – Dynamics and Scaling." *Quarterly of Applied Mathematics* 45 (3): 561–590.

Smith, G. P., D. M. Golden, M. Frenklach, N. W. Moriarty, B. Eiteneer, Mikhail Goldenberg, C. Thomas Bowman, Ronald K. Hanson, Soonho Song, William C. Gardiner, Jr, Vitali V. Lissianski, and Zhiwei Qin. *GRI-Mech 3.1*. http://www.me.berkeley.edu/grimech.

Sorensen, D., and A. Antoulas. 2002. "The Sylvester Equation and Approximate Balanced Reduction." *Linear Algebra and its Applications* 351–352(0): 671–700. doi: 10.1016/S0024-3795(02)00283-5.

Stefanescu, R., and I. M. Navon. 2013. "POD/DEIM Nonlinear Model Order Reduction of an ADI Implicit Shallow Water Equations Model." *Journal of Computational Physics* 237 (0): 95–114. doi: 10.1016/j.jcp.2012.11.035.

Stull, D. R., and H. Prophet. 1971. *JANAF Thermochemical Tables*. 2nded. Gaithersburg, MD: National Institute of Standards and Technology.

Wilson, G. J., and R. W. MacCormack. 1990. "Modeling Supersonic Combustion Using a Fully Implicit Numerical Method." *AIAA Journal* 30(4): 1008–1015. doi: 10.2514/3.11021.

Xiao, D., F. Fang, A. G. Buchan, C. C. Pain, I. M. Navon, J. Du, and G. Hu. 2014. "Non-Linear Model Reduction for the Navier-Stokes Equations Using Residual DEIM Method." *Journal of Computational Physics* 263(0): 1–18. doi: 10.1016/j.jcp.2014.01.011.

Young, T. R. 1980. *CHEMEQ – A Subroutine for Solving Stiff Ordinary Differential Equations* (NRL memorandum report 4091). Laboratory of Computational Physics, Naval Research Academy. Washington, D.C.

Young, T. R., and J. P. Boris. 1977. "A Numerical Technique for Solving Stiff Ordinary Differential Equations Associated with the Chemical Kinetics of Reactive-Flow Problems." *The Journal of Physical Chemistry* 81(25): 2424–2427. doi: 10.1021/j100540a018.